Investigation on seismic behavior of combined retaining structure with different rock shapes

Yu-liang Lin[*1,2,3], Lian-heng Zhao[**1], T.Y. Yang[2,4a], Guo-lin Yang[1b] and Xiao-bin Chen[1c]

[1]*School of Civil Engineering, Central South University, Changsha, 410075, China*
[2]*Department of Civil Engineering, University of British Columbia, Vancouver, V6T 1Z4, Canada*
[3]*State Key Laboratory for GeoMechanics and Deep Underground Engineering, China University of Mining & Technology, Xuzhou, 221008, China*
[4]*International Joint Research Laboratory of Earthquake Engineering, Tongi University, Shanghai, 200092, China*

Abstract. A combination of a gravity wall and an anchor beam is widely used to support the high soil deposit on rock mass. In this study, two groups of shaking table test were performed to investigate the responses of such combined retaining structure, where the rock masses were shaped with a flat surface and a curved surface, respectively. Meanwhile, the dynamic numerical analysis was carried out for a comparison or an extensive study. The results were studied and compared between the combined retaining structures with different shaped rock masses with regard to the acceleration response, the earth pressure response, and the axial anchor force. The acceleration response is not significantly influenced by the surface shape of rock mass. The earth pressure response on the combined retaining structure with a flat rock surface is more intensive than the one with a curved rock surface. The anchor force is significantly enlarged by seismic excitation with a main earthquake-induced increment at the first intensive pulse of Wenchuan motion. The value of anchor force in the combined retaining structure with a flat rock surface is generally larger than the one with a curved rock surface. Generally, the combined retaining structure with a curved rock surface presents a better seismic performance.

Keywords: gravity wall; anchor beam; shaped rock mass; shaking table test; numerical simulation

1. Introduction

In the past years, earthquakes frequently struck many countries in the world, which damaged numerous geotechnical structures, such as retaining structure, dam, slope, landslide, and embankment (Huang 2000, Singh *et al.* 2005, Bakir and Akis 2005, Xu *et al.* 2014, Kamai and Sangawa 2011). The great damage in earthquakes leads a demand for a well understanding on the behavior of geotechnical structure subjected to seismic excitation.

The stability of retaining structure and slope is a key issue in the field of geotechnical engineering, and a variety of analysis theories have been put forward or developed by scholars (Griffiths and Fenton 2004, Khajehzadeh *et al.* 2013, Aminpoor and Ghanbari 2014, Amipour *et al.* 2017, Zhou *et al.* 2019). However, when the earthquake loading is taken into consideration, the present seismic design adopts a quasi-static method for the seismic stability evaluation on retaining structure or slope, in which the dynamic earthquake loading is simplified as horizontal and vertical inertial forces (Greco 2001, Baker *et al.* 2006, Iskander *et al.* 2013). In spite of enormous research work conducted by many scholars for improving the quasi-static analysis method on the stability evaluation of retaining structure (Yang *et al.* 2014, Motlagh *et al.* 2014, Lin *et al.* 2017), the essential issues related to the dynamic response of retaining structure are still not well reflected due to the limitation of quasi-static method. To take account of the phase difference due to shear wave propagation, a more realistic pseudo-dynamic method is adopted by scholars to analyze the seismic stability of retaining structure and slope (Choudhury and Nimbalkar 2005, Shukha and Baker 2008, Zhou and Cheng 2014, Xu *et al.* 2017). Nevertheless, the theoretical approach is always developed under some certain assumptions. Dynamic centrifuge test and shaking table test are two effective ways to reveal a real dynamic response of retaining structure or slope. Jo *et al.* (2014, 2017) carried out centrifuge tests to investigate the earth pressure distribution as well as an influence of wall inertial force on a stiff inverted retaining wall. The results showed that the earth pressure presented a linear distribution under critical condition, and the inertial force influenced the moment of structure significantly. Tricarico *et al.* (2016) observed the dynamic response of cantilevered wall on saturated sand by dynamic centrifuge tests in terms of the acceleration and pore pressure in sand, the displacement

---

*Corresponding author, Associate Professor
 E-mail: linyuliang11@csu.edu.cn, linyuliang11@163.com
**Co-corresponding author, Professor
 E-mail: zlh8076@163.com
[a] Professor
 E-mail: yang@civil.ubc.ca
[b] Professor
 E-mail: yangguolin6301@163.com
[c] Professor
 E-mail: chen_xiaobin@csu.edu.cn

and bending moment of wall. Candia *et al*. (2016) studied the seismic response of a free-standing cantilever wall with a help of a series of sensors by dynamic centrifuge test, and the results of earth pressure on wall were compared with current design methods regarding the position of resultant force. Yazdandoust (2017, 2019a) assessed the performance of reinforced earth walls and MSE/soil nail hybrid retaining wall with different strip or nail length by 1-g shaking table test, and the observation indicated that the length strip or nail greatly influenced the deformation mode of walls. Meanwhile, the determination on horizontal seismic coefficient in different reinforced soil structures was analyzed based on the analytical and physical modeling (Yazdandoust 2019b). Latha and Santhanakumar (2015) carried out a shaking table test on the rigid modular reinforced walls, and the effects of soil density and reinforcement type on the behavior of rigid modular wall were analyzed. Suzuki *et al*. (2015) investigated the behavior of reinforced earth wall with different initial pullout loads, and drew a conclusion that the reinforced earth wall was greatly enhanced as a cement-treated soil was filled. Lin *et al*. (2018a, b) carried out groups of shaking table test on gravity retaining wall or sheet-pile wall with anchor beam to investigate their acceleration and earth pressure response.

A gravity wall combined with an anchor beam is one of the most widely used combined retaining structures for supporting the high slope in engineering practice. Nevertheless, the seismic design for such combined structure is still performed as that of a single-form retaining structure where the quasi-static or empirical methods are simply applied. The response of combined retaining structure under seismic excitation is much related to the geometric profile of supported soil or rock slope. In this study, two groups of shaking table test were carried out based on two adjacent cutting slope sections in DaRui Railway China that were supported by combined retaining structure. For these two cutting slope sections, the rock mass was shaped with a flat surface and a curved surface, respectively. A series of shaking cases were applied to investigate and compare the seismic response of combined retaining structures with different shaped rock masses by using shaking table model test and numerical analysis.

2. Shaking table test

The surface of rock mass was commonly shaped with different configurations by natural force, which might subsequently change the engineering behavior of geotechnical structure. A soil deposit on different shaped rock masses was supported by a combined retaining structure in two adjacent cutting slope sections in DaRui Railway of Yunnan Province, China. The rock mass was a kind of granitic gneiss with a weathered layer on the surface, and the soil deposit was an aggregate mixture of granite gravel and clay. The combined retaining structure constituted a gravity wall and an anchor beam. These two typical cutting slope sections showed a similar configuration except the main difference upon the surface

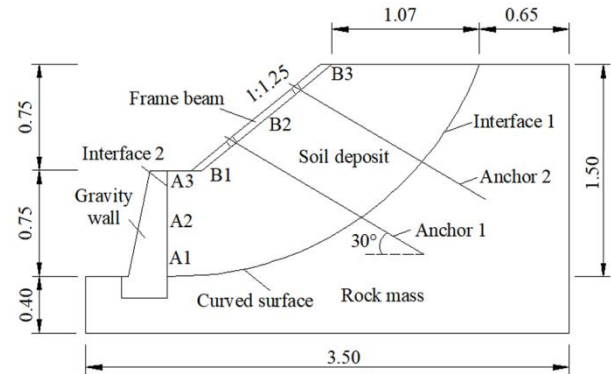Table 1 Similitude law for the main physical parameters in shaking table test

Physical parameters	Similitude law	Similitude ratio (Model/Prototype)
Length	S_l	1/8
Density	S_ρ	1
Cohesion	$S_c = S_\rho \cdot S_l$	1/8
Friction angle	S_φ	1
Stress	$S_\sigma = S_\rho \cdot S_l$	1/8
Acceleration	S_a	1
Acceleration time	$S_t = \sqrt{S_l / S_a}$	1/2.83
Frequency	$S_\omega = 1 / S_t$	1/0.35

shape of rock mass. For the prototype of the combined retaining structure with a flat rock surface, the surface of rock mass was inclined at 30.0° with the horizontal with a thin weathered rock layer between the rock mass and the soil deposit. As for the one with a curved rock surface, the rock mass was shaped as an arc curved surface with a radius of about 18.9 m. The arc curve was tangent to the horizontal surface at the bottom of gravity wall. The total length of flat interface was quite close to that of curved interface. The anchor was composed of steel bar with a diameter of 32 mm, and it was inclined at about 38.7° with the horizontal. Two rows of anchors linked the anchor beam to the rock mass with a 4.0 m anchoring length, and Anchors 1 and 2 were numbered upwards. Based on above two typical prototypes, the models of combined retaining structure were established in a 1:8 reduced scale in shaking table test, as presented in Fig.1. To apply a similitude relationship on the main physical and mechanical parameters between the model and the prototype, the similitude law was deduced by using the control variables of acceleration, density and geometric size based on the dimensional analysis of Buckingham π theorem. Subsequently, the similitude law for the main physical and mechanical parameters of model test was obtained, as shown in Table 1 (Wang and Lin 2011, Chen *et al*. 2015, Guler and Selek 2014).

Fig. 2 presented some photographs about the construction of combined retaining structure models. A model box (2.0 m high, 1.5 m wide, and 3.6 m long) was used to establish the shaking table models of combined retaining structure. The polystyrene foam was laid along the model box inside to decrease the seismic wave reflection on model boundary. To avoid a resonance between model box and shaking table model, two lateral sides of model box were rigidly supported to change its natural frequency (Lin *et al*. 2015, Fox *et al*. 2015). The rock mass, the gravity wall and the anchor beam in prototype had a high strength and a great stiffness, and they were not likely to fail in earthquake. Consequently, they were not the crucial issues that directly influenced the seismic stability of combined retaining structure. In similitude model, it was acceptable to construct a C25 concrete base at the bottom of model box to simulate the rock mass and the gravity wall. The flat surface and curved surface on rock mass were shaped with a help of special shuttering. A series of granite blocks were laid along
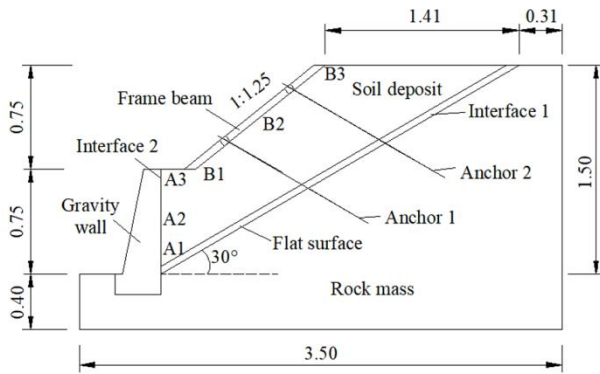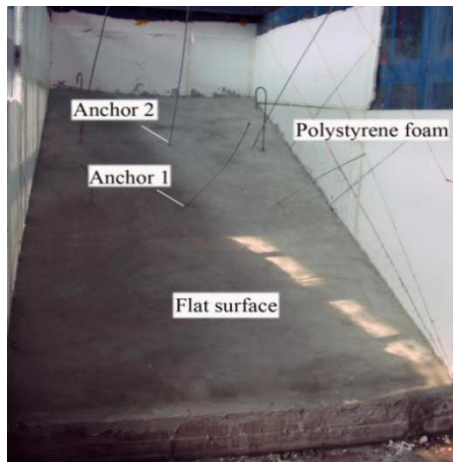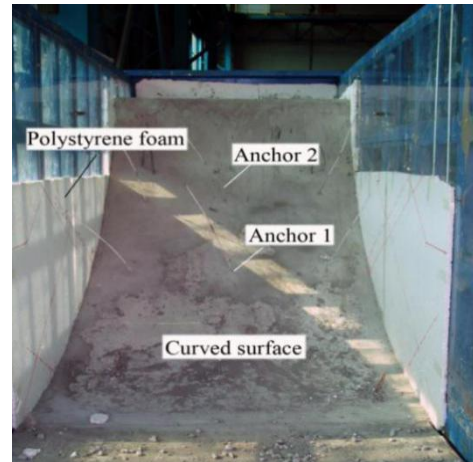
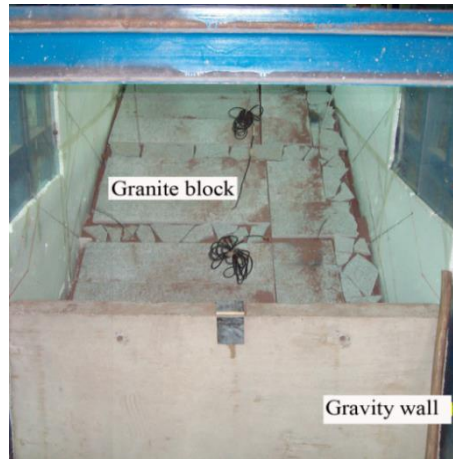(a) Rock mass with a flat surface (b) Rock mass with a curved surface

Fig. 1 The models of combined retaining structure supporting soil deposit on different shaped rock masses (Unit: m)
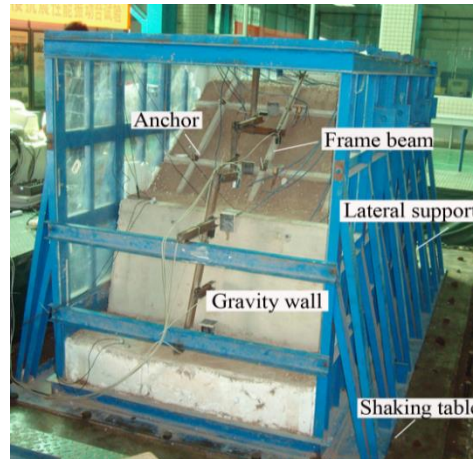

(a) Construction of flat rock surface (b) Construction of curved rock surface

(c) Construction of weathered layer (d) Wall face of combined retaining structure

Fig. 2 Photographs about the construction of combined retaining structure in shaking table tests.

the rock mass slope to simulate the weathered layer in the combined retaining structure with a flat rock surface. As for the soil deposit, the cohesion was very low, and the internal friction angle would dominate the strength issue. Since the similitude ratio for the internal friction angle was taken as 1.0, the aggregate mixture in slope prototype can be used in model test by sieving out the particles larger than 2cm. The internal friction angle and the cohesion of soil deposit were 34° and 6.2 kPa respectively based on triaxial test.

The compaction degree of soil deposit was about 93% in shaking table test. Based on similitude ratio of geometric size, the wires with 4 mm in diameter were adopted to simulate the anchors in combined retaining structure, and they were embedded into rock mass with a depth of 0.5 m. Due to a low cohesion of soil, the friction angle between the anchor and the soil would dominate the soil-anchor interaction. The frictional function between the anchor (wire) and the soil can well reflect the soil-anchor
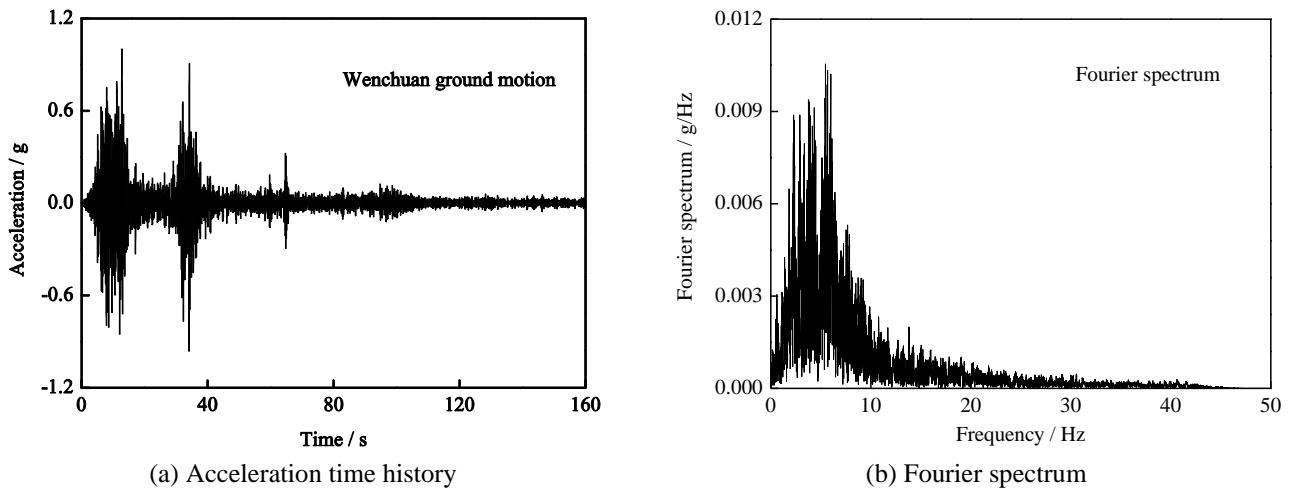
(a) Acceleration time history

(b) Fourier spectrum

Fig. 3 The acceleration time history and the Fourier spectrum of original Wenchuan motion

Table 2 Loading method of shaking table test

Serial number	Code-name	Peak input acceleration (g)	
		x	z
1	WN-1	0.03	0.03
2	WCXZ-1	0.10	0.067
3	WN-2	0.03	0.03
4	WCXZ-2	0.20	0.133
5	WN-3	0.03	0.03
6	WCXZ-3	0.40	0.267
7	WN-4	0.05	0.05
8	WCXZ-4	0.60	0.40

interaction in prototype since a 1:1 similitude ratio of friction angle is adopted in similitude law.

Wenchuan motion in 2008 China Wenchuan Earthquake was bi-directionally applied (in horizontal and vertical directions, represented by x and z) in the form of acceleration time history in shaking table test (see Fig. 3(a)). Subsequently, the loading rate was only dependent on the frequency of seismic ground motion. It was seen that the predominant frequency of Wenchuan motion mainly concentrated at a low frequency range of 0.5-8.0 Hz (see Fig. 3(b)). Corresponding to earthquake fortification intensities of VII, VIII, IX and >IX, the acceleration of Wenchuan motion in x-direction was scaled at four levels: 0.1, 0.2, 0.4, and 0.6 g. The acceleration in z-direction was adjusted to 2/3 of that in x-direction for every shaking case, as shown in Table 2. The White Noise cases were imposed among the shaking cases in shaking table tests.

3. Numerical simulation

The prototypes of combined retaining structure were derived from two adjacent cutting slope sections with different shaped rock masses in DaRui Railway, China. Accordingly, the 1:1 numerical models of combined retaining structure were established by using FLAC3D code (see Fig. 4). In FLAC3D platform, the static models and parameters are applicable for dynamic analysis according to FLAC3D manual. From the perspective of algorithm, the

essence of FLAC3D is to solve the equation of motion. When it comes to a static analysis, a special damping is used to make the calculation converge more quickly. Under a certain occasion, the static method of FLAC3D is also called as a pseudo-dynamic method, which makes it possible to perform a dynamic analysis by using static models and parameters (Ghiasi and Mozafari 2018, Abuhajar *et al*. 2015, Ertugrul 2016). On the other hand, the predominant frequency of seismic ground motion mainly concentrates at a low frequency band. The dynamic mechanical parameters under a low frequency range are quite close to that in static state. Therefore, the values of the main mechanical parameters of combined retaining structure in static state are mainly given in this study.

To make a reasonable comparison, each component of these two numerical models was simulated by the same method in FLAC3D software, and was attached with the same physical and mechanical parameters. According to the geotechnical test results and the geological data of prototypes, the main parameters for the combined retaining structures in prototype were shown in Table 3. To simulate a potential slippage behavior, two interfaces were established at some special positions in combined retaining structures. One interface element was set between the rock mass and the soil deposit (named Interface 1), and the other one was established between the gravity wall and the soil deposit (named Interface 2). It was noted that the Interface 1 in the combined retaining structure with a flat rock surface was a flat surface inclined at 30° with the horizontal, and in the one with a curved rock surface, it was an arc surface with a curve radius of 18.9 m. Based on shear test and engineering geological data, the stiffness of Interfaces 1 and 2 were 570 and 855 GPa/m respectively. The friction angle of Interface 1 is 18.0° and the cohesion was neglected, and they were 23.8° and 3.1 kPa for Interface 2. A structural element of "cable" provided by FLAC3D software was used to simulate the anchors in combined retaining structures, by which it was convenient to attach corresponding values for different parameters of anchor, such as the density, the tensile strength, the compressive strength, the bond strength, and so on. The "cable" was one of two-node

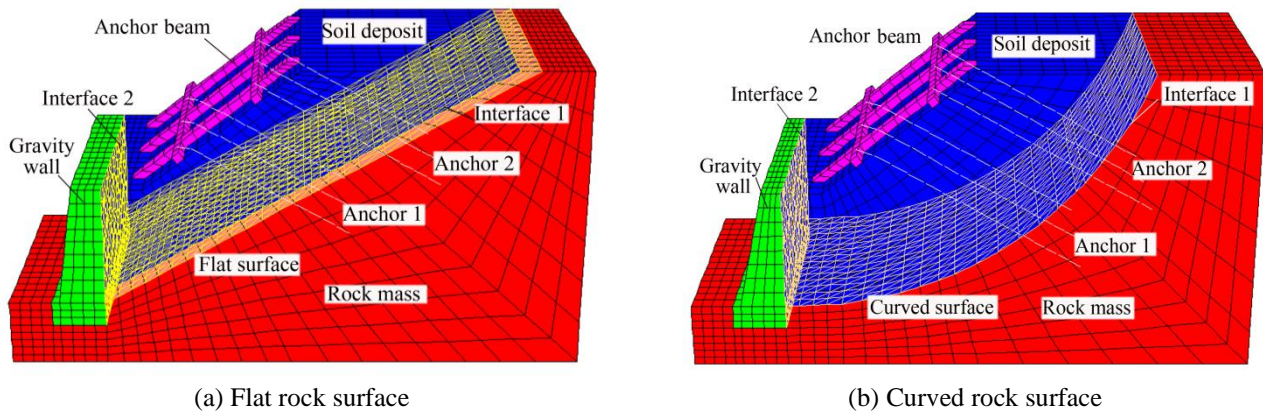(a) Flat rock surface (b) Curved rock surface

Fig. 4 Numerical models of combined retaining structures with flat rock surface and curved rock surface

Table 3 The main model parameters of combined retaining structure in numerical analysis

Items	Model	Density (kg/m^3)	Bulk modulus (MPa)	Shear modulus (MPa)	Cohesion (kPa)	Frictional angle (°)
Soil deposit	M-C	1960	72.7	17.3	6.2	34
Gravity wall	Elastic	2500	17857	12295	/	/
Anchor beam	Elastic	2500	16071	11066	/	/
Rock mass	Elastic	2600	18056	13542	/	/

Table 4 The geometric length of anchors in combined retaining structures (Unit: m)

Combined retaining structure	length of Anchor 1 in free part	length of Anchor 1 in anchoring part	Total length of Anchor 1	length of Anchor 2 in free part	length of Anchor 2 in anchoring part	Total length of Anchor 2
Flat surface	5.3	4.0	9.3	6.1	4.0	10.1
Curved surface	8.4	4.0	12.4	8.1	4.0	12.1

Table 5 The main parameters of anchor in dynamic numerical analysis

Items	Model	Density (kg/m^3)	Elastic modulus (MPa)	Tensile strength (kPa)	Compressive strength (kPa)	Grout cohesive strength with soil (MN/m)	Grout friction angle with soil (°)	Grout cohesive strength with rock (MN/m)	Grout friction anglewith rock (°)	Stiffness with rock (MPa)
Anchor	Cable	2,400	22,000	310	310	≈0	11	1.2	18	21.0

structural element, and it was possible to check the axial force of anchor at different axial locations. The geometric length of anchor in combined retaining structures with different shaped rock mass was shown in Table 4. The "cable" structural element adopts the grout cohesive strength and the grout friction angle to reflect the interaction strength between the anchor and the soil or the rock. Table 5 showed the values of main parameters of anchor in prototype. According to engineering geological data and empirical value, the grout cohesive strength between the anchor and the rock was given as 1.2 MN/m, where the cohesive strength would dominate the whole interaction strength. The grout friction angle of 11°, which was about 1/3 of soil internal friction angle, was attached between the anchor and the soil deposit, and the grout cohesive strength was neglected.

A Free Field Method was taken to decrease the seismic reflection on the boundary of numerical models. Free grid elements were generated by which an infinite boundary condition was established. The Local Damping was adoptedfor damping setting of combined retaining structures because the Local Damping could reach a satisfactory result in dynamic numerical analysis without

any negative effect on dynamic calculation time step. Additionally, the first 50 s of original Wenchuan motion was applied in numerical analysis to speed up the computing time without changing the basic characteristic of Wenchuan motion.

4. Result and analysis

4.1 Horizontal acceleration response

The response of acceleration is a crucial issue for the seismic evaluation on geotechnical structure. For example, the widely used quasi-static method in present seismic design takes the basic information of acceleration amplification distribution to determine the horizontal and vertical inertiaforces. Fig. 5 presents the horizontal acceleration (*x*-direction) against time for several test points in combined retaining structures with different shaped rock masses subjected to WCXZ-2 shaking case. The curve of acceleration response against time presents a similar shape as that of Wenchuan motion. However, the intensity of

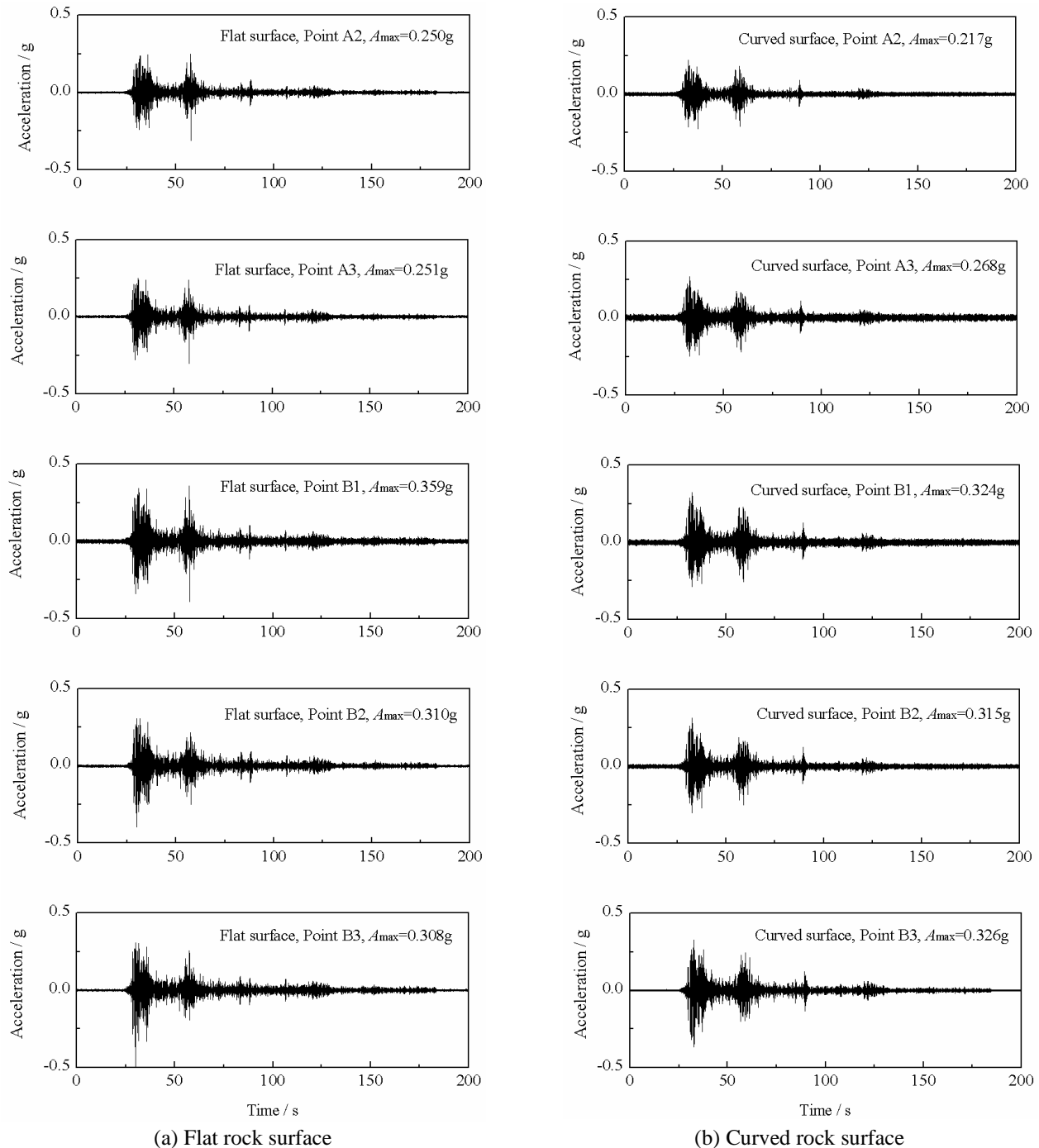(a) Flat rock surface   (b) Curved rock surface

Fig. 5 Time history of acceleration response for several points in combined retaining structure with flat rock surface and curved rock surface

acceleration response is largely amplified. Taking the combined retaining structure with a flat rock surface for example, as the horizontal acceleration of seismic excitation reaches 0.20 g (i.e., WCXZ-2 shaking case), the peak acceleration response for Points A2 and B1 increase to 0.250 g and 0.359 g, respectively. The peak acceleration response increases with an increase in elevation behind gravity wall, while it does not show obvious increasing tendency along the height of anchor beam. Apart from that, Point B1 shows more intensive acceleration response than Point A3 although these two test points are at a same

elevation. Consequently, it is indicated that the toe of anchor beam is more vulnerable to seismic excitation, and it demands a special strengthening in engineering design. The above phenomenon is observed in both the combined retaining structure with a flat rock surface and the one with a curved rock surface. Subsequently, it is concluded that the time history of acceleration response in *x*-direction is not so significantly affected by the surface shape of rock mass.

The acceleration amplification, a ratio of tested peak acceleration to the one at the toe of gravity wall, is commonly used to analyze the amplification effect on the

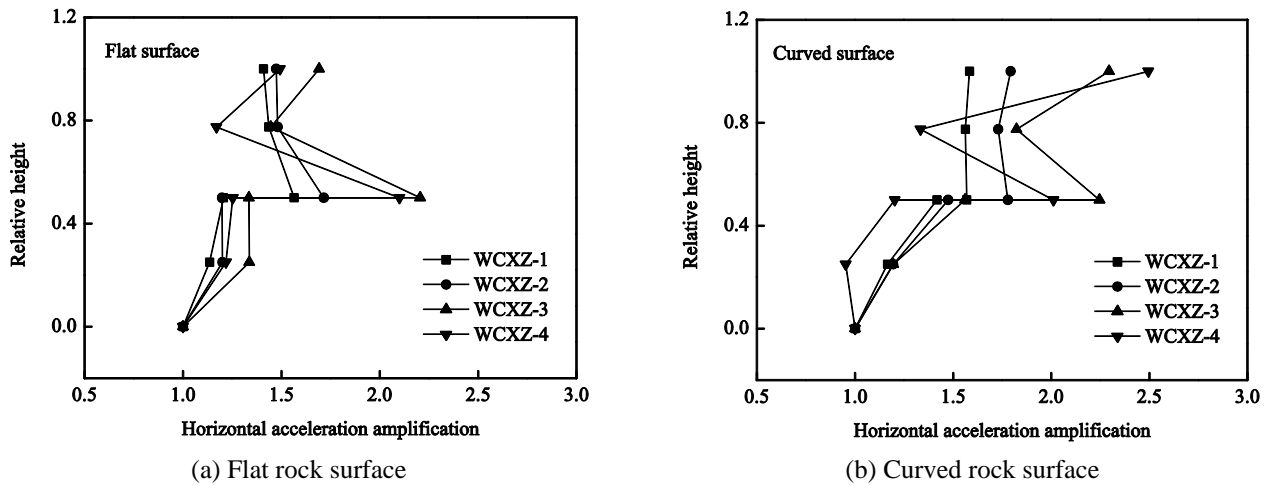(a) Flat rock surface   (b) Curved rock surface

Fig. 6 The distribution of horizontal acceleration amplification for combined retaining structures with flat rock surface and curved rock surface in shaking table test
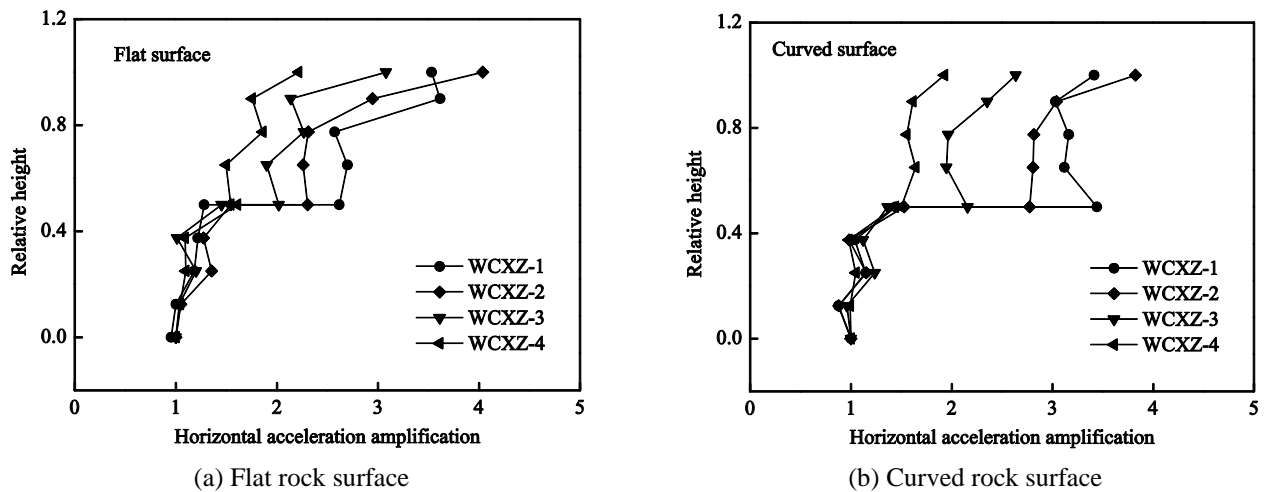

(a) Flat rock surface   (b) Curved rock surface

Fig. 7 The distribution of horizontal acceleration amplification for combined retaining structures with flat rock surface and curved rock surface in dynamic numerical analysis

acceleration response of retaining structure. Figs. 6 and 7 compare the horizontal acceleration amplification distribution for the combined retaining structures with different shaped rock masses subjected to different shaking cases in shaking table test and numerical analysis. Where, the relative height denotes a dimensionless parameter determined by dividing the elevation of test point by the height of combined retaining structure (H=12 m). Along the height of gravity wall, the horizontal acceleration amplification presents an increasing tendency. At 0.5 relative height, the horizontal acceleration amplification presents a sharp increment, which corresponds with the above observation that Point B1 shows a much more intensive acceleration response than Point A3. Generally, the horizontal acceleration amplification at anchor beam is much larger than that of gravity wall. The difference of horizontal acceleration amplification is not so obvious between the combined retaining structure with a flat rock surface and the one with a curved rock surface.

The observation from shaking table test shows that the horizontal acceleration amplification becomes more irregular at the upper structure of combined retaining structure (i.e. anchor beam) as the input acceleration in *x*-direction increases (See shaking cases of WCXZ-3 and WCXZ-4 in Fig. 6). The phenomenon indicates that the combined retaining structure presents a more significant nonlinearity while the input acceleration in *x*-direction is larger than 0.4 g.

The numerical analysis results illustrate that the horizontal acceleration amplification of anchor beam shows a decreasing tendency as the intensity of seismic excitation increases (see Fig. 7), which is not obviously observed in shaking table test. Probably the soil slope below the anchor beam tends to be more compacted after the shaking case in shaking table test, which may even induce an increasing acceleration amplification due to a greater soil stiffness. However, a further study is still required to make a more convincing interpretation for such discrepancy. The observation from numerical analysis seems to be more reasonable because the anchor beam tends to dissipate more seismic energy while experiencing a strong ground motion. A similar conclusion is also observed in the previous

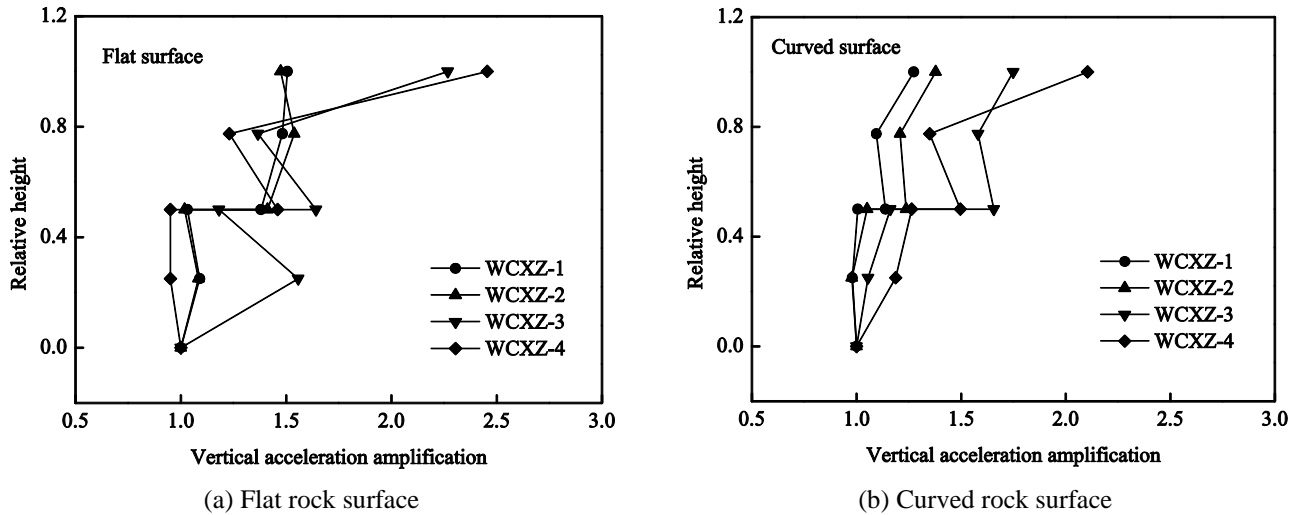(a) Flat rock surface   (b) Curved rock surface

Fig. 8 Distribution of vertical acceleration amplification of combined retaining structures with flat rock surface and curved rock surface in shaking table test
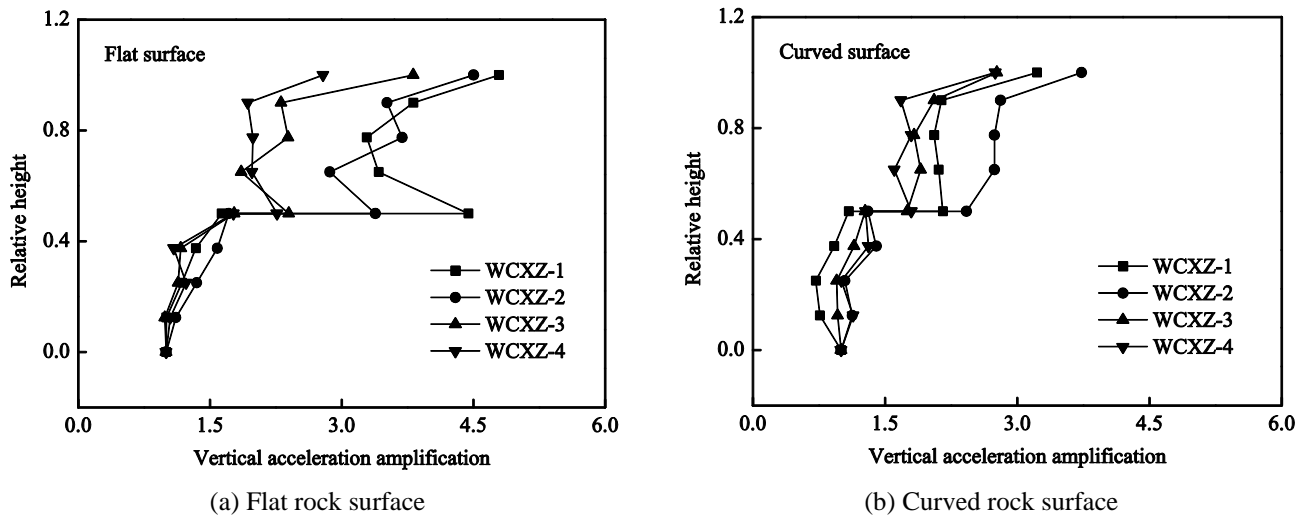

(a) Flat rock surface   (b) Curved rock surface

Fig. 9 Distribution of vertical acceleration amplification of combined retaining structures with flat rock surface and curved rock surface in dynamic numerical analysis

published paper with regard to the correlation between the acceleration magnification and the intensity of seismic excitation for soil slope (Lin *et al.* 2015).

4.2 Vertical acceleration response

Fig. 8 shows the vertical acceleration amplifications (*z*-direction) of combined retaining structures with different shaped rock masses in shaking table test, and the numerical analysis results are shown in Fig. 9. Some common results are observed in both shaking table tests and numerical analysis. With an increase in elevation behind the gravity wall and the anchor beam, the vertical acceleration amplification presents an increasing tendency. Similar to the results in *x*-direction, the vertical acceleration amplification presents a significant increment at 0.5 relative height, which indicates that a special reinforcement is also required at the toe of anchor beam in z-direction. Besides, there is no great

difference between the combined retaining structures with different shaped rock masses regarding the vertical acceleration amplification. The acceleration response in z-direction is not obviously affected by the surface shape of rock mass either.

The vertical acceleration amplification of anchor beam seems to be more scattered than that of gravity wall subjected to shaking cases of WCXZ-3 and WCXZ-4 (see Fig. 8), which is consistent with the observation of the acceleration amplification in *x*-direction. Subsequently, it is inferred that a more significant nonlinearity appears at the upper structure of combined retaining structure in both horizontal and vertical directions. The results derived from numerical analysis indicate that the vertical acceleration amplification of anchor beam tends to decrease as the intensity of seismic excitation increases (see Fig. 9) because the anchor beam dissipates more and more seismic energy. However, the shaking table test does not present an obvious correlation between the vertical acceleration amplification

(a) Point A1, Flat surface

(b) Point A1, Curved surface

(c) Point A2, Flat surface

(d) Point A2, Curved surface

(e) Point A3, Flat surface
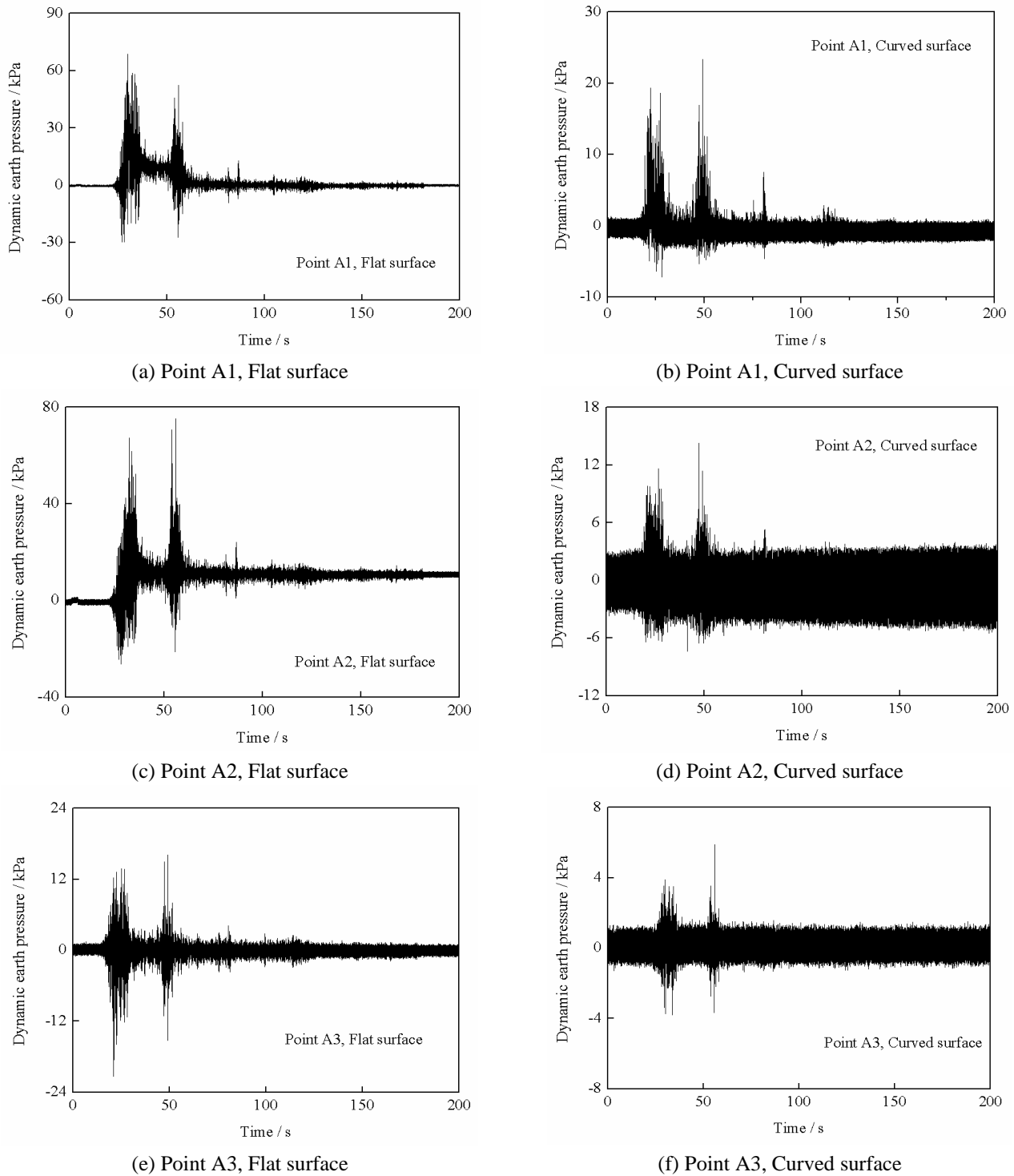

(f) Point A3, Curved surface

Fig. 10 Response of dynamic earth pressure of combined retaining structures with different shaped rock mass under WCXZ-4 shaking case in shaking table test.

and the intensity of seismic excitation due to a data dispersion.

4.3 Earth pressure response

The response of dynamic earth pressure behind the rigid lower structure of combined retaining structure (i.e. gravity wall) is mainly discussed here. The static earth pressure is removed to solely study the dynamic earth pressure caused by seismic excitation. Fig. 10 presents the response of dynamic earth pressure of the combined retaining structures with different shaped rock masses under shaking case of WCXZ-4 in shaking table test. In which, Points A1, A2 and A3 are at different elevations of gravity wall (see Fig. 1). The distribution of peak value of dynamic earth pressure along the height of gravity wall is shown in Fig. 11. Generally, the intensity of dynamic earth pressure response
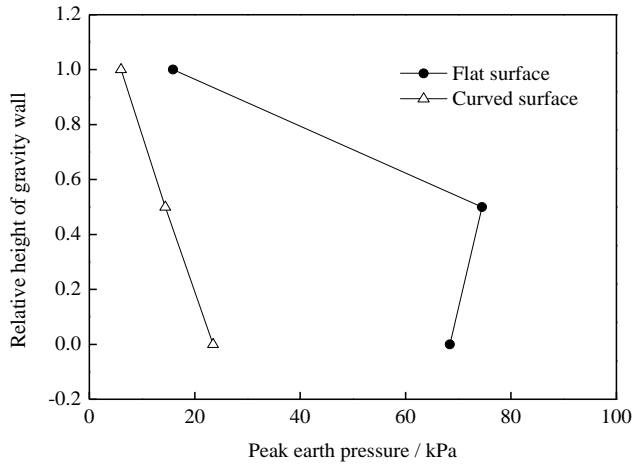
Fig. 11 Distribution of peak value of earth pressure response along the height of gravity wall

Table 6 The maximum axial anchor force in combined retaining structures with different rock shapes (Unit: kPa)

Shaking cases	Flat surface		Curved surface	
	Anchor 1	Anchor 2	Anchor 1	Anchor 2
Static	14	10	12	8
WCXZ-1	53	28	21	9
WCXZ-2	177	86	68	29
WCXZ-3	Yield	260	300	156
WCXZ-4	Yield	Yield	Yield	280

decreases with an increase in elevation behind the gravity wall, and it is the most intensive around the toe of gravity wall. The phenomenon is observed in both the combined retaining structure with a flat rock surface and the one with a curved rock surface. Apart from that, the different characteristics of dynamic earth pressure response observed between these two combined retaining structures are concluded as follows.

(a) The baseline of earth pressure response behind the combined retaining structure with a flat rock surface presents two obvious offsets under shaking case of WCXZ-4. The endpoint of baseline does not come to naught after the shaking case, which means an increment of residual earth pressure behind the gravity wall. For instance, the increment of residual earth pressure for Point E2 in the combined retaining structure with a flat rock surface is 11.2 kPa under shaking case of WCXZ-4. It is not appropriate to neglect such a large earthquake-induced residual earth pressure behind the gravity wall. The increment of residual earth pressure in *x*-direction may greatly decrease the seismic stability of retaining structures. However, for the combined retaining structure with a curved rock surface, the baseline offset of dynamic earth pressure response is not so obvious. Consequently, it seems like that the combined retaining structure with a flat rock surface is more vulnerable to the seismic excitation than the one with a curved rock surface regarding the dynamic earth pressure response behind the gravity wall. Additionally, it is noted that such increment of residual earth pressure due to earthquake loading is not involved in present seismic design theory, such as the widely used Mononobe-Okabe theory, which is required to be modified for making a more reasonable seismic design of retaining structure.

(b) The response of dynamic earth pressure on the combined retaining structure with a flat rock surface is much more intensive than the one with a curved rock surface. For instance, the maximum values of dynamic earth pressure at Points A1, A2 and A3 in the combined retaining structure with a flat rock surface are 68.8 kPa, 75.2 kPa and 16.2 kPa respectively, while they are 23.4 kPa, 14.6 kPa and 5.9 kPa in the combined retaining structure with a curved

rock surface (see Fig. 11). The ratios for these three points are 2.94:1, 5.15:1 and 2.74:1 respectively between these two combined retaining structures with different shaped rock masses.

4.4 Axial anchor force

The upper structure of combined retaining structure (i.e. anchor beam) is linked to the rock mass by anchors. Consequently, the anchors play a crucial role regarding the stability of combined retaining structure. The axial anchor force is also a main issue in seismic design of such combined retaining structure.

Fig. 12 compares the distributions of axial anchor force between the combined retaining structures with different shaped rock masses in numerical analysis. Where, "static" denotes a static condition without any shaking case, and the axial anchor force in this condition is caused by gravity; "Free part" refers to the anchor section buried in soil deposit; And "anchoring part" refers to the anchoring section in rock mass. The maximum values of axial anchor force in these two combined retaining structures subjected to different shaking cases are shown in Table 6. The distribution of axial anchor force shows some common characteristics in the combined retaining structures with different shaped rock masses. The axial force of Anchor 1 presents a double-peak distribution, where one of peak axial anchor force (the maximum one) exists next to the anchor head that was fixed with anchor beam. The other one occurs near the position between the anchoring part and the free part. The force distribution of Anchor 2 presents a sing-peak characteristic where the maximum anchor force appears in the middle of free part. The axial anchor force decreases rapidly around the interface between the anchoring part and the free part, and it approaches naught within a short length in anchoring part. A larger axial anchor force is investigated in Anchor 1 than in Anchor 2. For example, in the combined retaining structure with a curved rock surface, the maximum value of axial force of Anchor 1 is 68 kPa under WCXZ-2 shaking case, and it is 29 kPa for Anchor 2, only about 42.6% of Anchor 1.

The value of axial anchor force in the combined retaining structure with a flat rock surface is generally larger than the one with a curved rock surface. Taking Anchor 1 for example, the maximum value of anchor force is about 177 kPa in the combined retaining structure with a flat rock surface subjected to WCXZ-2 shaking case, and it is only about 68 kPa in the one with a curved rock surface.

(a) Flat surface, Anchor 1

(b) Curved surface, Anchor 1

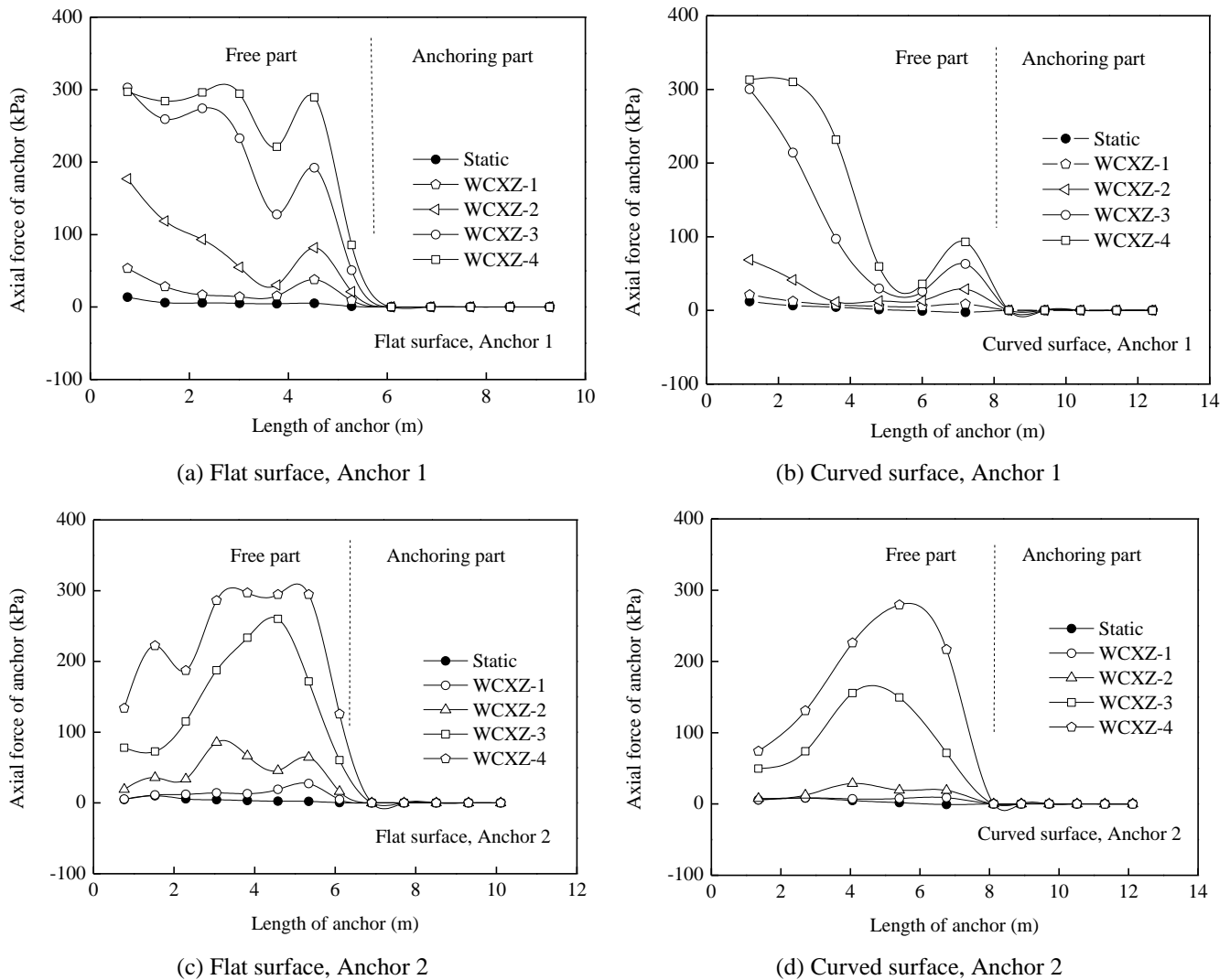(c) Flat surface, Anchor 2

(d) Curved surface, Anchor 2

Fig. 12 The distributions of axial anchor force in combined retaining structures with different shaped rock mass

As the horizontal acceleration of seismic excitation increases to 0.4g (under WCXZ-3 shaking case), the force of Anchor 1 reaches its yield strength of 310 kPa in the combined retaining structure with a curved rock surface (see Table 6). Thereafter, more and more sections of Anchor 1 get close to its yield strength in free part as the input acceleration increases (e.g. Fig. 12(a)).

The axial anchor force changes along the axial position. The position with the maximum axial anchor force is selected to analyze the time history of anchor force response. Fig. 13 shows the maximum axial anchor force response against time in the combined retaining structures with different shaped rock masses under different shaking cases. The baseline of axial force response does not return to zero even when the shaking case has finished, which reflects an earthquake-induced increment of axial anchor force. Besides, it is seen that the axial anchor force is mainly enlarged by the first intensive pulse of Wenchuan motion. The Anchor 1 in the combined retaining structure with a flat rock surface has already approached its yield strength due to the first intensive pulse of Wenchuan motion

under WCXZ-3 shaking case (See Fig. 13 (e)). The axial anchor force tends to be quite stable while the structure experiences the second intensive pulse of Wenchuan motion. It is obvious that the axial anchor force in the combined retaining structure with a flat rock surface is much larger than the one with a curved rock surface. In terms of the mechanical behavior of anchor, it is seen that the combined retaining structure with a curved rock surface presents a better seismic performance.

5. Conclusions

The acceleration responses are amplified subjected to seismic excitation, and a more intensive amplification effect is observed near the toe of anchor beam. The response behavior of acceleration along the wall face of combined retaining structure is not obviously affected by the surface shape of rock mass. The acceleration amplification of the upper structure of combined retaining structure becomes more irregular as the intensity of seismic excitation increases.
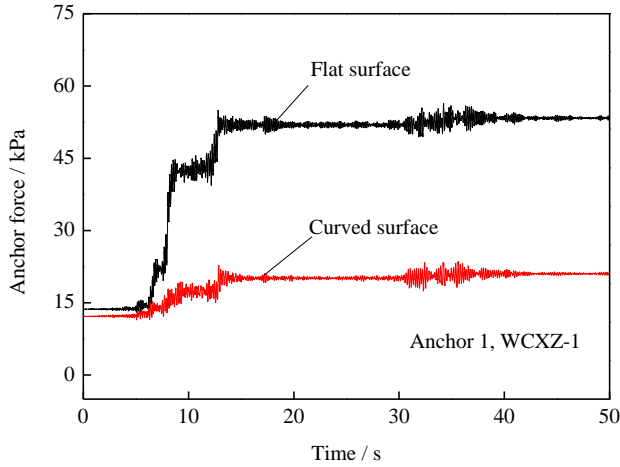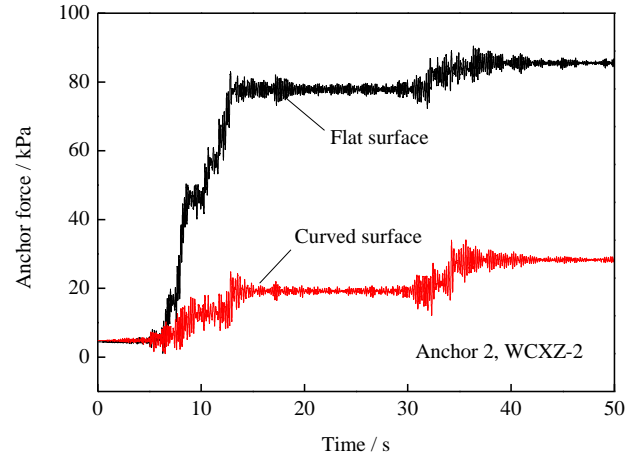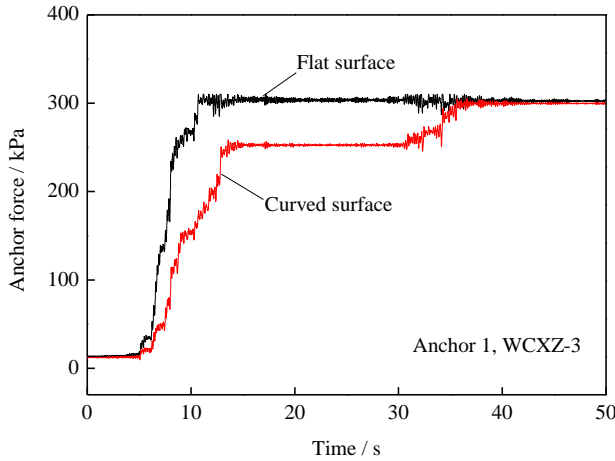
(a) Anchor 1, WCXZ-1 shaking case
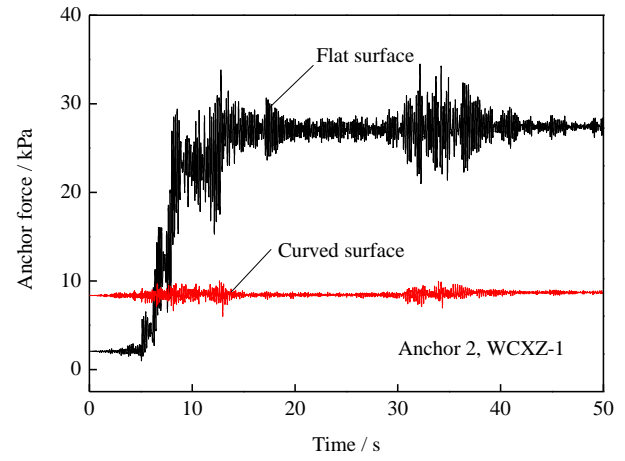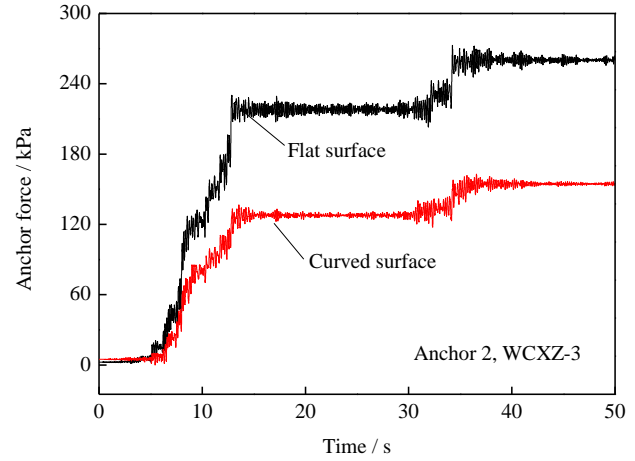
(b) Anchor 2, WCXZ-1 shaking case
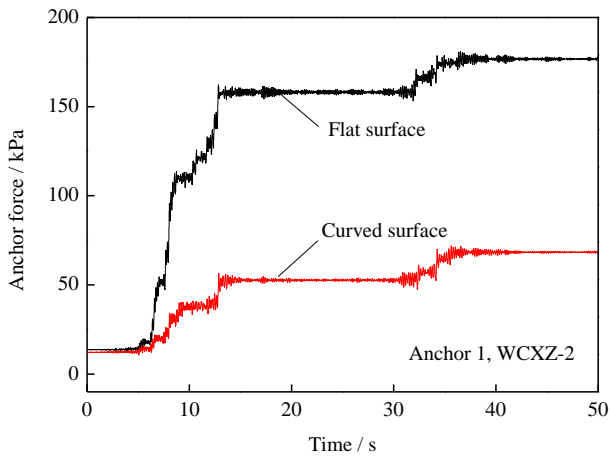
(c) Anchor 1, WCXZ-2 shaking case

(d) Anchor 2, WCXZ-2 shaking case

(e) Anchor 1, WCXZ-3 shaking case

(f) Anchor 2, WCXZ-3 shaking case

Fig. 13 The maximum axial anchor force response between the combined retaining structures with different shaped rock masses under different shaking cases

The response of dynamic earth pressure around the toe of gravity wall is the most intensive. The residual earth pressure on the gravity wall is obviously enlarged by earthquake loading. The response of dynamic earth pressure on the combined retaining structure with a flat rock surface is more intensive than that behind the one with a curved rock surface.

The axial anchor force is significantly enlarged by earthquake loading. The axial anchor force is mainly enlarged by the first intensive pulse of Wenchuan motion. A larger anchor force is investigated in Anchor 1 than in Anchor 2. The axial anchor force in the combined retaining structure with a flat rock surface is generally larger than the

one with a curved rock surface. The combined retaining structure with a curved rock surface presents a better seismic performance.

Acknowledgement

References

Abuhajar, O., El Naggar, H. and Newson, T. (2015), "Seismic soil-culvert interaction", *Can. Geotech. J.,* **52**(11), 1649-1667.https://doi.org/10.1139/cgj-2014-0493.

Aminpoor, M.M. and Ghanbari, A. (2014), "Design charts for yield acceleration and seismic displacement of retaining walls with surcharge through limit analysis", *Struct. Eng. Mech.,* **52**(6): 1225-1256. https://doi.org/10.12989/sem.2014.52.6.1225.

Aminpour, M.M., Maleki, M. and Ghanbari, A. (2017), "Investigation of the effect of surcharge on behavior of soil slopes", *Geomech. Eng.,* **13**(4), 653-669. https://doi.org/10.12989/gae.2017.13.4.653.

Bakir, B.S. and Akis, E. (2005), "Analysis of a highway embankment failure associated with the 1999 Duzce, Turkey earthquake", *Soil Dyn. Earthq. Eng.,* **25**(3), 251-260. https://doi.org/10.1016/j.soildyn.2003.05.001.

Baker, R., Shukha, R., Operstein, V. and Frydman, S. (2006), "Stability charts for pseudo-static slope stability analysis", *Soil Dyn. Earthq. Eng.,* **26**(9), 813-823. https://doi.org/10.1016/j.soildyn.2006.01.023.

Candia, G., Mikola, R.G. and Sitard, N. (2016), "Seismic response of retaining walls with cohesive backfill: Centrifuge model studies", *Soil Dyn. Earthq. Eng.,* **90**, 411-419. https://doi.org/10.1016/j.soildyn.2016.09.013.

Chen, G., Chen, S., Zuo, X., Du, X., Qi, C. and Wang, Z. (2015), "Shaking-table tests and numerical simulations on a subway structure in soft soil", *Soil Dyn. Earthq. Eng.,* **76**, 13-28. https://doi.org/10.1016/j.soildyn.2014.12.012.

Choudhury, D. and Nimbalkar, S. (2005), "Seismic passive resistance by pseudo-dynamic method", *Geotechnique,* **55**(9), 699-702. https://doi.org/10.1680/geot.2005.55.9.699.

Ertugrul, O.L. (2016), "Numerical modeling of the seismic racking behavior of box culverts in dry cohesionless soils", *KSCE J. Civ. Eng.,* **20**(5), 1737-1746. https://doi.org/10.1007/s12205-015-0235-1.

Fox, P.J., Sander, A.C., Elgamal, A., Greco, P., Isaacs, D., Stone, M. and Wong, S. (2015), "Large soil confinement box for seismic performance testing of geo-structures", *Geotech. Test. J.,* **38**(1), 72-84. https://doi.org/10.1520/GTJ20140034.

Ghiasi, V. and Mozafari, V. (2018), "Seismic response of buried pipes to microtunnelling method under earthquake loads", *Soil Dyn. Earthq. Eng.,* **113**, 193-201. https://doi.org/10.1016/j.soildyn.2018.05.020.

Greco, V.R. (2001), "Pseudo-static thrust on cantilever walls", *Soils Found.,* **41**(3), 87-92. https://doi.org/10.3208/sandf.41.3_87.

Griffiths, D.V. and Fenton, G.A. (2004), "Probabilistic slopes tability analysis by finite elements", *J. Geotech. Geoenviron.,* **130**(5), 507-518. https://doi.org/10.1061/(ASCE)1090-0241(2004)130:5(507)

Guler, E. and Selek, O. (2014), "Reduced-scale shaking table tests on geosynthetic-reinforced soil walls with modular racing", *J. Geotech. Geoenviron.,* **140**(6), 04014015. https://doi.org/10.1061/(ASCE)GT.1943-5606.0001102.

Huang, C.C. (2000), "Investigations of soil retaining structures damaged during the Chi-Chi (Taiwan) earthquake", *J. Chin. Inst. Eng.,* **23**(4), 417-428. https://doi.org/10.1080/02533839.2000.9670562.

Iskander, M., Chen, Z., Omidvar, M., Guzman, I. and Elsherif, O. (2013), "Active static and seismic earth pressure for c-psi soils", *Soils Found.,* **53**(5), 639-652. https://doi.org/10.1016/j.sandf.2013.08.003.

Jo, S.B., Ha, J.G., Lee, J.S. and Kim, D.S. (2017), "Evaluation of the seismic earth pressure for inverted T-shape stiff retaining wall in cohesionless soils via dynamic centrifuge", *Soil Dyn. Earthq. Eng.,* **92**, 345-357. https://doi.org/10.1016/j.soildyn.2016.10.009.

Jo, S.B., Ha, J.G., Yoo, M., Choo, Y.W. and Kim, D.S. (2014), "Seismic behavior of an inverted T-shape flexible retaining wall via dynamic centrifuge tests", *B. Earthq. Eng.,* **12**(2), 961-980. https://doi.org/10.1007/s10518-013-9558-9.

Kamai, T. and Sangawa, A. (2011), "Landslides on ancient embankments in the Kinki district (Japan): Strong motion seismoscope of the 1596 Keichou-Fushimi earthquake", *Quatern. Int.,* **242**(1), 90-105. https://doi.org/10.1016/j.quaint.2011.04.002.

Khajehzadeh, M., Taha, M.R. and Eslami, M. (2013), "Efficient gravitational search algorithm for optimum design of retaining walls", *Struct. Eng. Mech.,* **45**(1), 111-127. https://doi.org/10.12989/sem.2013.45.1.111

Latha, G.M. and Santhanakumar, P. (2015), "Seismic response of reduced-scale modular block and rigid faced reinforced walls through shaking table tests", *Geotext. Geomembr.,* **43**(4), 307-316. https://doi.org/10.1016/j.geotexmem.2015.04.008.

Lin, Y.L., Cheng, X.M. and Yang, G.L. (2018a), "Shaking table test and numerical simulation on a combined retaining structure response to earthquake loading", *Soil Dyn. Earthq. Eng.,* **108**, 29-45. https://doi.org/10.1016/j.soildyn.2018.02.008.

Lin, Y.L., Cheng, X.M., Yang, G.L. and Li, Y. (2018b), "Seismic response of a sheet-pile wall with anchoring frame beam by numerical simulation and shaking table test", *Soil Dyn. Earthq. Eng.,* **115**, 352-364. https://doi.org/10.1016/j.soildyn.2018.07.028.

Lin, Y.L., Yang, X., Yang, G.L., Li, Y. and Zhao, L.H. (2017), "A closed-form solution for seismic passive earth pressure behind a retaining wall supporting cohesive-frictional backfill" *Acta Geotech.,* **12**(2): 453-461. http:// doi.org/10.1007/s11440-016-0472-6

Lin, Y.L., Leng, W.M., Yang, G.L., Li, L. and Yang, J.S. (2015), "Seismic response of embankment slopes with different reinforcing measures in shaking table tests", *Nat. Hazards,* **76**(2), 791-810. https://doi.org/10.1007/s11069-014-1517-5.

Motlagh, A.T., Ghanbari, A., Maedeh, P.A. and Wu, W. (2018), "A new analytical approach to estimate the seismic tensile force of geosynthetic reinforcement respect to the uniform surcharge of slopes", *Earthq. Struct.,* **15**(6), 687-699. https://doi.org/10.12989/eas.2018.15.6.687.

Nian, T.K., Liu, B., Han, J. and Huang, R.Q. (2014), "Effect of seismic acceleration directions on dynamic earth pressures in retaining structures", *Geomech. Eng.,* **7**(3), 263-277. https://doi.org/10.12989/gae.2014.7.3.263.

Savalle, N., Vincens, E. and Hans, S. (2018), "Pseudo-static scaled-down experiments on dry stone retaining walls: Preliminary implications for the seismic design", *Eng. Struct.,* **171**, 336-347. https://doi.org/10.1016/j.engstruct.2018.05.080.

Shukha, R. and Baker, R. (2008), "Design implications of the vertical pseudo-static coefficient in slope analysis", *Comput. Geotech.*, **35**(1), 86-96. https://doi.org/10.1016/j.compgeo.2007.01.005.

Singh, R., Roy, D. and Jain, S.K. (2005), "Analysis of earth dams affected by the 2001 Bhuj Earthquake", *Eng. Geol.*, **80**(3-4), 282-291. https://doi.org/10.1016/j.enggeo.2005.06.002.

Suzuki, M., Shimura, N., Fukumura, T., Yoneda, O. and Tasaka, Y.(2015), "Seismic performance of reinforced soil wall with untreated and cement-treated soils as backfill using a 1-g shaking table", *Soils Found.*, **55**(3), 626-636. https://doi.org/10.1016/j.sandf.2015.04.013.

Temur, R. and Bekdas, G. (2016), "Teaching learning-based optimization for design of cantilever retaining walls", *Struct. Eng. Mech.*, **57**(4): 763-783. https://doi.org/10.12989/sem.2016.57.4.763.

Tricarico, M., Madabhushi, G.S.P. and Aversa, S. (2016), "Centrifuge modelling of flexible retaining walls subjected to dynamic loading", *Soil Dyn. Earthq. Eng.,* **88**, 297-306. https://doi.org/10.1016/j.soildyn.2016.06.013.

Wang, K.L. and Lin, M.L. (2011), "Initiation and displacement of landslide induced by earthquake - a study of shaking table model slope test", *Eng. Geol.,* **122**, 106-114. https://doi.org/10.1016/j.enggeo.2011.04.008.

Xu, C., Xu, X.W., Yao, X. and Dai, F.C. (2014), "Three (nearly) complete inventories of landslides triggered by the May 12, 2008 Wenchuan Mw 7.9 earthquake of China and their spatial distribution statistical analysis", *Landslides*, **11**(3): 441-461. https://doi.org/10.1007/s10346-013-0404-6.

Xu, X., Zhou, X.P., Huang, C.X. and Cu, L.Q. (2017), "Wedge-failure analysis of the seismic slope using the pseudo dynamic method", *Int. J. Geomech.*, **17**(12), 04017108. https://doi.org/10.1061/(ASCE)GM.1943-5622.0001015.

Yang, C.W., Zhang, J.J., Fu, X., Zhu, C.B. and Bi, J.W. (2014), "Improvement of pseudo-static method for slope stability analysis", *J. Mt. Sci-Engl.*, **11**(3), 625-633. https://doi.org/10.1007/s11629-013-2756-8.

Yazdandoust, M. (2017), "Investigation on the seismic performance of steel-strip reinforced-soil retaining walls using shaking table test", *Soil Dyn. Earthq. Eng.,* **97**, 216-232. https://doi.org/10.1016/j.soildyn.2017.03.011.

Yazdandoust, M. (2019a), "Shaking table modeling of MSE/soil nail hybrid retaining walls", *Soils Found*, **59**(2): 241-252. https://doi.org/10.1016/j.sandf.2018.05.013.

Yazdandoust, M. (2019b), "Assessment of horizontal seismic coefficient for three different types of reinforced soil structure using physical and analytical modeling", *Int J Geomech*, **19**(7): 04019070. https://doi.org/10.1061/(ASCE)GM.1943-5622.0001344.

Zhou, X.P. and Cheng, H. (2014), "Stability analysis of three-dimensional seismic landslides using the rigorous limit equilibrium method", *Eng. Geol.*, **174**, 87-102. https://doi.org/10.1016/j.enggeo.2014.03.009.

Zhou, X.P., Zhu, B.Z., Juang, C.H. and Wong, L.N.Y. (2019), "A stability analysis of a layered-soil slope based on random field", *B. Eng. Geol. Environ.*, **78**(4), 2611-2625. https://doi.org/10.1007/s10064-018-1266-x.

PL